High-pressure structural and dielectric studies of the phase transitions in lithium thallium tartrate monohydrate

2002 J. Phys.: Condens. Matter 14 4045

(http://iopscience.iop.org/0953-8984/14/15/318)

INSTITUTE OF PHYSICS PUBLISHING JOURNAL OF PHYSICS: CONDENSED MATTER

J. Phys.: Condens. Matter **14** (2002) 4045–4054 PII: S0953-8984(02)32770-X

High-pressure structural and dielectric studies of the phase transitions in lithium thallium tartrate monohydrate

S Kamba[1], J Kulda[2], V Petříček[1], G McIntyre[2] and J P Kiat[3]

[1] Institute of Physics, Academy of Sciences of the Czech Republic, Na Slovance 2, 18221 Prague 8, Czech Republic
[2] Institute Laue-Langevin, BP 56, 38042 Grenoble Cedex 9, France
[3] Laboratoire de Chimie-Physique du Solide (URA 453 au CNRS), Ecole Centrale, F-92215 Chatenay-Malabry Cedex, France

E-mail: kamba@fzu.cz

Received 16 January 2002, in final form 20 March 2002
Published 4 April 2002
Online at stacks.iop.org/JPhysCM/14/4045

Abstract

We have investigated the structure of lithium thallium tartrate monohydrate ($LiTlC_4H_4O_6{\cdot}H_2O$) single crystal by means of neutron diffraction at a hydrostatic pressure of 120 MPa. Atomic positions including those of hydrogen atoms have been refined for the orthorhombic paraelectric phase ($P2_12_12$) at 36 K and for the monoclinic ferroelectric (FE) phase ($P2_111$) at 6 K. Moreover, our dielectric results, confirmed by the temperature variation of the monoclinic splitting, provide evidence for the existence of an intermediate FE phase in the temperature range between $T_{c'} = 24$ K and $T_c = 34$ K. The two FE phases are probably isomorphous but differ in their degree of monoclinic distortion and in their value of the piezoelectric coefficients. Both phase transition temperatures drop with decreasing hydrostatic pressure and only a single FE phase is observed below 11 K at ambient pressure. The spontaneous polarization appears along the crystallographic axis a and, according to our structure data, it can be mainly attributed to displacements of the Li atoms accompanied by a realignment of crystal-water molecules.

1. Introduction

Lithium thallium tartrate monohydrate (LTT)—$LiTlC_4H_4O_6{\cdot}H_2O$—in its paraelectric (PE) phase has a similar crystal structure (space group $P2_12_12$–D_2^3, $Z = 4$) [1–3] to the Rochelle salt (RS) $NaKC_4H_4O_6{\cdot}4H_2O$, which was the first ferroelectric (FE) discovered [4]. The RS exhibits, however, a lattice parameter along the $\boldsymbol{a}$-axis that is almost twice as long and hosts four crystal-water molecules, all due to the much larger radius of the sodium ion as compared to the lithium in LTT. It is not surprising that the dielectric behaviours of the two materials

as regards temperature change are different. RS exhibits a (FE) phase (monoclinic space group $P2_111$–C_2^2, $Z = 4$, $\boldsymbol{P}_s \parallel \boldsymbol{a}$ [1]) only in a relatively narrow temperature range between $T_{C1} = 255$ K and $T_{C2} = 297$ K [4]. LTT undergoes only one proper ferroelectric phase transition (FPT) at $T_c = 11$ K [5], which is the lowest known T_c among all stoichiometric FEs. The temperature dependence of dielectric permittivity $\varepsilon'_a(T)$ of this compound is similar to that in incipient FEs or quantum PEs, and a plateau is seen below 11 K [6, 7]. Difficulties with the measurements of dielectric hysteresis loops [8] can be explained by large quantum fluctuations of polarization below T_c. The LTT is piezoelectric already in the PE phase and it was shown that close to T_c both the elastic compliance s_{44}^E and the piezoelectric coefficient d_{14} reach the highest magnitude measured in any material [7]. The piezoelectric effect is also responsible for a large (two orders of magnitude) difference between the free and clamped dielectric permittivities [7, 9, 10].

T_c for LTT decreases with the degree of deuteration and vanishes in highly deuterated crystals [11, 12]. A substantial increase in T_c with hydrostatic pressure was observed in dielectric and Raman scattering experiments [13] and T_c reached 55 K at 380 MPa. Note that KDP and all other hydrogen-bonded FEs exhibit the opposite behaviour, i.e. a decrease of T_c with increasing hydrostatic pressure and/or deuteration [14]. The temperature dependence of ε'_a exhibits an unusual shape at high pressures—a broad plateau appears in $\varepsilon'_a(T)$ below T_c. The width of this plateau depends on pressure: at 5–15 K below T_c (let us denote this temperature as $T_{c'}$), ε'_a drops steeply to about half of its value. An optical phonon, which incompletely softens from 21 cm^{-1} at 300 K down to 9 cm^{-1} at T_c and hardens below T_c, was observed in both FIR and Raman spectra [13, 15]. It gives evidence of the displacive character of the phase transition (PT). However, no phonon anomaly has been seen at $T_{c'}$. The plateau in $\varepsilon'_a(T)$ was explained by the domain wall motion contribution to ε'_a and the step down in ε'_a at $T_{c'}$ by domain wall freezing [13]. This conclusion follows also from FE hysteresis loop measurements [13], where slim hysteresis loops were observed in the plateau region ($T_{c'} < T < T_c$) and the polarization was not switchable below $T_{c'}$.

Microscopic insight into these effects cannot be gained without knowledge of the low-temperature structure of the FE phase, so far lacking. The aim of the present work is to fill up this gap.

2. Experimental procedure

The samples were prepared from the same LTT single crystal, grown from aqueous solution [11] and having a volume of several cubic centimetres, as the samples used in our previous study [13]. The complex dielectric function $\varepsilon^* = \varepsilon' - \mathrm{i}\varepsilon''$ was obtained in the temperature region 25–300 K using a Wayne–Kerr B905 A and a Keithley 3322 automatic bridge operating under computer control, at frequencies $f = 0.1$, 0.4, 1, 10 kHz and $f = 0.5$, 1, 5, 10, 50, and 100 kHz, respectively. Hydrostatic pressure up to 380 MPa was achieved in a custom-made gas pressure cell with helium as a pressure medium by means of a NOVA compressor combined with a hand pump.

Prior to the neutron diffraction experiment on the single crystal, the temperature dependence of the lattice parameters had been determined at ambient pressure down to 6.5 K using x-rays. The x-ray source was a rotating anode (18 kW) with a high-resolution two-axis goniometer (Bragg–Brentano geometry), using an InP backward monochromator selecting the Cu K$\alpha_1 = 1.540\,562$ Å wavelength, permitting one to achieve an accuracy of 4×10^{-6} Å in determination of the lattice parameters. A helium cryostat with precision and stability of 0.1 K down to 10 K and stability of 0.5 K between 6.5 and 10 K was used. Lattice parameters a and b were both measured for a virgin powder sample.

The neutron diffraction data were obtained on the hot-neutron diffractometer D9 at the Institut Laue-Langevin. The Cu 220 monochromator in combination with a $\lambda/2$ filter was used to select neutrons with wavelengths of about 0.84 Å. An attempt to obtain the FE phase structure at ambient pressure has been undertaken, using a continuous-flow helium cryostat in the four-circle mode. As the FE displacements proved to be too small to be resolved, the decisive part of the experiment was undertaken at high pressure, permitting us to pass deeper into the FE phase. The sample of $2.5 \times 2.5 \times 3$ mm^3 was placed in a copper–beryllium clamped cell loaded to 150 MPa. The data were collected in two-circle mode using a lifting detector arm. The applied pressure of 120 ± 10 MPa at 30 K was determined from the temperatures of observed diffraction anomalies compared with high-pressure dielectric anomalies. Datasets consisting of 2258 and 1688 reflections have been collected at the respective temperatures of 6 and 36 K. The structure parameters of LTT were refined from the diffraction data using the JANA98 program [16].

3. Experimental results and discussion

The temperature dependences of the lattice parameters a and b, obtained by means of x-ray powder diffraction at ambient pressure, are displayed in figure 1. Both parameters reveal a classical Debye behaviour down to $T_c = 11$ K, where small positive jumps of 9×10^{-4} (a-parameter) and 3.5×10^{-5} Å (b-parameter) appear and than the lattice parameters remain constant down to the lowest measured temperature, 6.3 K. Note that the jumps in lattice parameters are abnormal because they are positive. The jumps also give information about the weak first-order nature of the PT. After heating to room temperature, both lattice parameters return to slightly higher values (see figure 1) probably due to the sublimation of crystal-water from the powder samples. This was why the measurements of both lattice parameters were performed on virgin samples.

The neutron diffraction measurement was started at 300 K and ambient pressure and the data agreed very well with those already published in [3]. The room temperature structure was also checked after cooling and it was confirmed that no change was observed. The FE structure was studied at 2.5 K; however, no significant change between the PE and FE phases was observed. In particular, the monoclinic distortion was so small in the FE phase that it could not be resolved in our data.

Therefore we repeated the neutron diffraction measurement at an applied hydrostatic pressure of 120 ± 10 MPa to increase the T_c so that the experiment could be performed deeper in the FE phase with a more significant FE distortion. Indeed, below 35 K the monoclinic splitting of the $0k0$ reflections is readily observed; as an example, figure 2 displays the (0, 12, 0) reflection at 38 and 6 K. From the temperature dependence of the splitting in figure 3(b) we can see that the monoclinic angle α varies from 90.048° at 28 K to 90.183° at 6 K. The temperature $T_c = 35$ K, at which the splitting of several reflections appears, corresponds to the high-temperature anomaly in permittivity and to the soft-mode frequency minimum (cf figure 3). This temperature was already interpreted in [13] as the FPT temperature. The second dielectric anomaly at $T_{c'} = 24$ K, attributed in [13] to the freezing of FE domains, coincides with the change in the temperature dependence of the Bragg reflection splitting in figure 3(b); hence this anomaly seems to indicate another PT to an isomorphous monoclinic phase. Unfortunately, we do not have enough Raman data near $T_{c'}$ at 120 MPa, but from the Raman measurement at higher pressures [13] we know that the soft-mode frequency does not exhibit any anomaly near $T_{c'}$.

The structure of the PE phase at 36 K was refined using the orthorhombic $P2_12_12$ space group. An agreement factor $R = 4.66\%$ was reached for the final solution with 78 structural

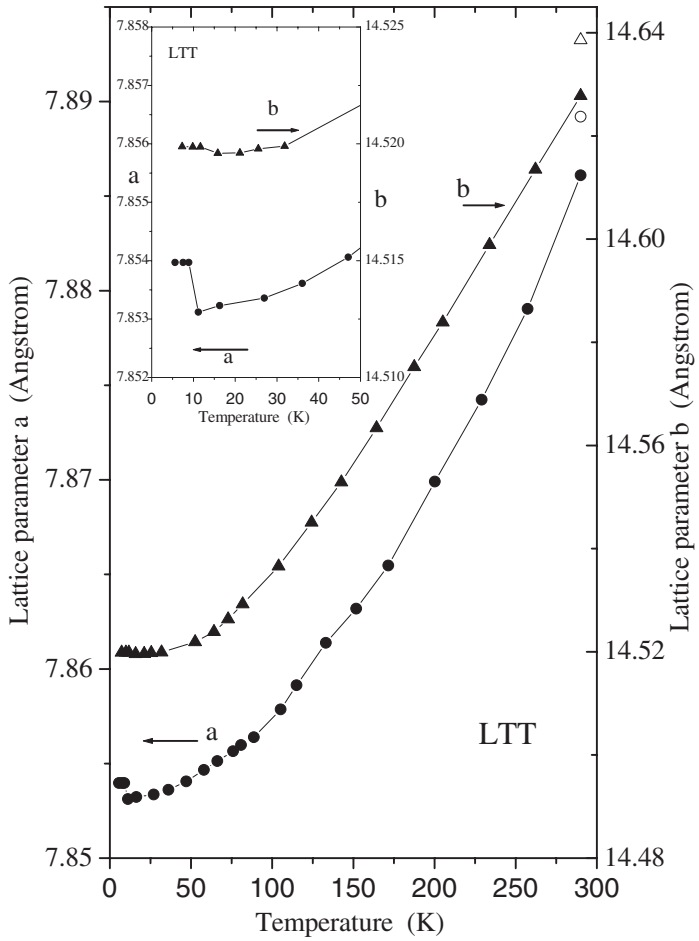

Figure 1. Temperature dependences of lattice parameters obtained from the x-ray powder diffraction on cooling at ambient pressure. Open symbols show lattice parameters at RT measured after heating up.

parameters from 716 independent observed reflections. The resulting positional parameters, displayed in table 1 and in figure 4, correspond to the previously established room temperature structure reported in [3]. For the low-temperature (6 K) data, refinements using both the orthorhombic $P2_12_12$ and the monoclinic $P2_111$ space groups were attempted. Although the changes of atomic positions between the FE and PE phases (6 and 36 K) are relatively small, the refinement of 98 parameters from 1631 reflections ($R = 4.99\%$), using a twinned model, has confirmed the splitting of the unit cell due to the disappearing 2_1 axis along the b-direction. Contrary to the case for the RS [17], the $0k0$ reflections with k odd remain almost insignificant in the PE phase. This indicates that the disappearance of the 2_1 axis along the b-axis, needed to bring about the spontaneous polarization along the a-axis, is due almost exclusively to the atom displacements along the a-axis. As seen in table 1, the most significant displacements are found for the Li ions along the a-direction, accompanied by reorientation of the H_2O molecules. Nevertheless, it seems that hydrogen atoms do not play an essential role in driving the FPT, since no increase of T_c with deuteration in LTT was observed [11, 12]. We have

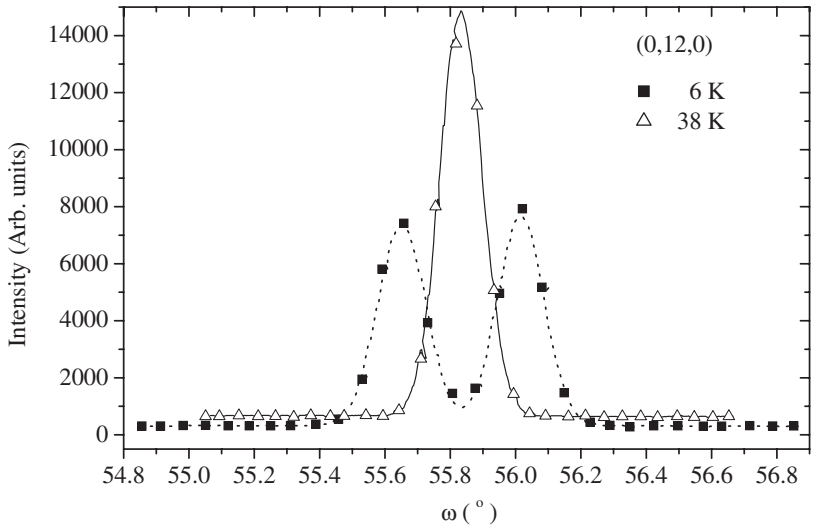

Figure 2. The (0, 12, 0) Bragg reflection profiles (ω-scan) observed at 38 and 6 K under an applied pressure of 120 MPa.

also observed that the water molecules exhibit a noticeable rotation already in the PE phase between 300 and 36 K without creating any spontaneous polarization. So we may conclude that Li ions probably play the main role at the FPT in LTT. The problem can, however, be more complex and also small shifts of other atoms can contribute to the polarization.

In an effort to understand the phases below T_c, the high-pressure dielectric data partially published in [13] were re-evaluated. The temperature dependences of ε'_a obtained at five different hydrostatic pressures at selected frequencies are shown in figure 5. The increase in both T_c and $T_{c'}$ with pressure is clearly seen; the phase diagram was published in [13]. In ε'_a, practically no dependence is seen below 10 kHz; however, strong dependence is seen at higher frequencies up to 100 kHz at temperatures where a plateau in ε'_a appears. Unfortunately, the measurements up to 100 kHz were performed only at 50 and 115 MPa; at higher pressures a Wayne–Kerr B905 bridge (instead of a Keithley 3322) was used and it allowed measurement only up to 10 kHz. The enhanced ε'_a appears due to the strong piezoelectric coupling already seen in [9] at ambient pressure and low temperature. The piezoelectric coupling depends on the sample thickness; therefore a different (lower) value of ε'_a was observed for a 194 μm thick sample (figure 6). The ε'_a obtained for our two samples are partially clamped; the free permittivity reaches values of the order of 10^3 below T_c (at ambient pressure); the clamped permittivity has a value of about 30 only [9, 15]. The thinner the sample, the higher the clamping, which occurs due to the electrodes. The applied voltage 1 V used in the dielectric measurement is rather high, but we checked that the same values of ε'_a were obtained at a voltage of 50 mV—essentially only the noise was higher. In our case we measure ε'_a, which is closer to the free-permittivity value (see figure 5) and the change of ε'_a at $T_{c'}$ can occur only due to change of the piezoelectric resonance. In consequence of the absence of any anomaly of the low-lying optical soft mode near $T_{c'}$, the change in clamped permittivity resulting from the polar phonon contribution is negligible.

One could ask whether the change in free permittivity at $T_{c'}$ does not arise due to some artificial effect, for example a clamping of the sample as a consequence of helium solidification (helium was used as a pressure medium). However, we have shown already in [13] that the

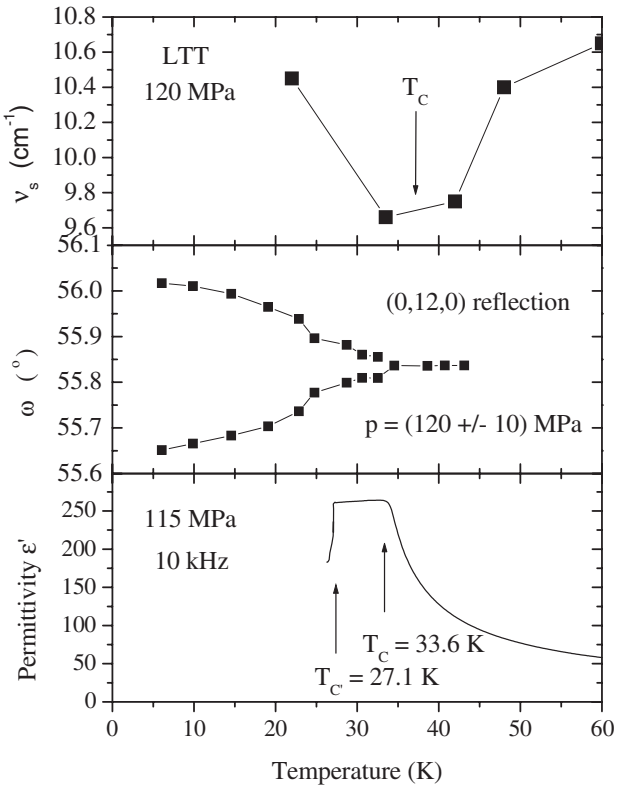

Figure 3. Temperature dependences of (*a*) the FE soft-mode frequency ν_s observed in the $b(cb)c$ Raman spectra at 120 MPa (after [13]), (*b*) the splitting of the (0, 12, 0) Bragg reflection at 120 MPa (the accuracy is $\pm 0.01^\circ$), and (*c*) the permittivity ε'_a at 115 MPa.

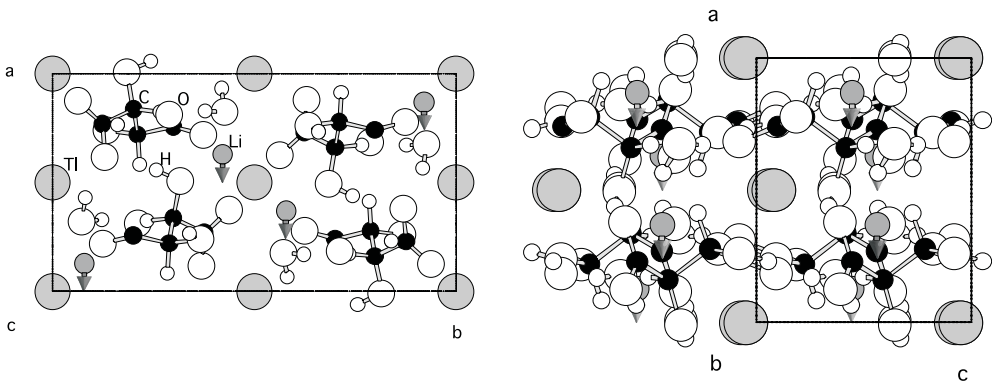

Figure 4. Projections of the LTT unit cell at 38 K along the *c*- and *b*-directions. The arrows indicate the displacements of the Li ions in the low-temperature FE phase.

helium melts at 15 K (at 120 MPa), which is 12 K lower than $T_{c'}$. Moreover, at the same $T_{c'}$ we also see an anomaly in the splitting of the (0, 12, 0) reflection (figure 3(*b*)) and in this case another pressure medium (oil) was used. It is hard to imagine another artifact; therefore we conclude that the change in the free ε'_a at $T_{c'}$ can arise only due to the sudden change of the

Table 1. A list of the atomic positions in LTT crystal at 120 MPa and at 36 and 6 K. The first line corresponds to the orthorhombic refinement for 36 K and the second one to the monoclinic refinement for 6 K. The last column gives the distance difference between those two positions.

Atom	x	y	z	Δ (Å)
Tl1	0	0	0.947 6(3)	
	0	−0.003 4(2)	0.947 0(2)	0.050(3)
Tl2	0	0.5	0.923 2(3)	
	0.005(3)	0.497 5(2)	0.923 2(2)	0.056(18)
Li1a	0.129 973	0.078 7	0.441 4(3)	
	0.109(7)	0.079 4(11)	0.449 (3)	0.18(5)
Li1b	−0.129 973	−0.078 7	0.441 4(3)	
	−0.139(7)	−0.078 2(9)	0.435 (2)	0.09(5)
C1a	0.258(5)	0.200 7(5)	0.095 7(12)	
	0.255(2)	0.201 51(14)	0.092 8(3)	0.03(3)
C2a	0.221(5)	0.289 0(5)	0.219 9(12)	
	0.221(2)	0.290 0(2)	0.216 3(5)	0.028(15)
C3a	0.338 2(13)	0.299 17(11)	0.413 5(2)	
	0.333(2)	0.298 9(2)	0.412 5(5)	0.04(2)
C4a	0.269 5(13)	0.376 12(11)	0.557 5(2)	
	0.269(2)	0.376 9(2)	0.554 0(5)	0.025(4)
O1a	0.220(2)	0.125 1(2)	0.181 3(5)	
	0.215(2)	0.126 0(2)	0.178 0(5)	0.05(2)
O2a	0.314(2)	0.211 4(2)	−0.085 5(5)	
	0.319(2)	0.211 4(2)	−0.086 5(5)	0.04(2)
O3a	0.374(2)	0.437 3(2)	0.612 1(4)	
	0.374(2)	0.437 4(2)	0.610 8(7)	0.009(7)
O4a	0.119(2)	0.369 7(2)	0.617 3(4)	
	0.116(2)	0.372 6(3)	0.610 9(6)	0.065(11)
O5a	0.239(2)	0.366 0(2)	0.086 0(4)	
	0.243(2)	0.367 2(2)	0.081 6(6)	0.046(18)
O6a	0.507(2)	0.316 0(2)	0.357 0(4)	
	0.507(2)	0.313 9(3)	0.360 4(7)	0.038(5)
H1a	0.266(2)	0.339 8(2)	−0.049 4(5)	
	0.273(2)	0.339 7(3)	−0.052 4(8)	0.06(2)
H2a	0.559(2)	0.256 4(2)	0.335 3(5)	
	0.557(2)	0.253 4(4)	0.342 1(10)	0.063(8)
H3a	0.086(2)	0.284 3(2)	0.276 7(5)	
	0.086(2)	0.286 5(3)	0.267 0(9)	0.070(7)
H4a	0.326(2)	0.234 2(2)	0.504 0(5)	
	0.321(2)	0.234 9(3)	0.504 7(7)	0.04(2)
C1b	−0.258(2)	−0.200 7(2)	0.095 7(5)	
	−0.257(2)	−0.200 26(14)	0.098 8(3)	0.022(9)
C2b	−0.221(2)	−0.289 0(2)	0.219 9(5)	
	−0.219(2)	−0.287 7(2)	0.225 1(5)	0.043(12)
C3b	−0.338(2)	−0.299 2(2)	0.413 5(5)	
	−0.338(2)	−0.298 8(2)	0.415 5(5)	0.014(7)

Table 1. (Continued.)

Atom	x	y	z	Δ (Å)
C4b	−0.270(2)	−0.376 1(2)	0.557 5(5)	
	−0.273(2)	−0.375 0(2)	0.56 1 2(5)	0.038(18)
O1b	−0.220(2)	−0.125 1(2)	0.181 3(5)	
	−0.225(2)	−0.123 8(2)	0.184 9(5)	0.05(2)
O2b	−0.314(2)	−0.211 4(2)	−0.085 5(5)	
	−0.313(2)	−0.211 9(2)	−0.083 6(5)	0.017(14)
O3b	−0.374(2)	−0.437 3(2)	0.612 1(5)	
	−0.374(2)	−0.437 7(2)	0.613 5(7)	0.010(5)
O4b	−0.119(2)	−0.369 7(2)	0.617 3(5)	
	−0.121(2)	−0.367 1(3)	0.625 9(6)	0.070(9)
O5b	−0.239(3)	−0.366 0(3)	0.086 0(8)	
	−0.231(2)	−0.365 5(2)	0.090 5(6)	0.07(3)
O6b	−0.507(3)	−0.316 0(3)	0.357 0(8)	
	−0.508(2)	−0.317 8(3)	0.354 7(8)	0.032(12)
H1b	−0.266(4)	−0.339 8(4)	−0.049 4(9)	
	−0.259(2)	−0.339 1(3)	−0.045 3(8)	0.06(3)
H2b	−0.559(4)	−0.256 4(4)	0.335 3(9)	
	−0.563(2)	−0.258 6(4)	0.333 0(10)	0.05(2)
H3b	−0.086(3)	−0.284 3(4)	0.276 7(10)	
	−0.087(2)	−0.281 0(3)	0.282 7(9)	0.063(11)
H4b	−0.326(3)	−0.234 2(4)	0.504 0(10)	
	−0.333(3)	−0.234 4(3)	0.507 3(7)	0.07(3)
O7a	0.323(4)	0.072 8(3)	0.637 5(7)	
	0.322(2)	0.071 6(3)	0.641 9(9)	0.035(13)
H5a	0.329(4)	0.122 0(3)	0.744 8(7)	
	0.322(3)	0.118 4(6)	0.754 3(16)	0.09(2)
H6a	0.433(3)	0.081 5(3)	0.561 0(6)	
	0.418(3)	0.089 2(8)	0.557 (2)	0.17(2)
O7b	−0.323(3)	−0.072 8(3)	0.637 5(6)	
	−0.329(2)	−0.074 3(3)	0.633 5(9)	0.06(2)
H5b	−0.329(5)	−0.122 0(6)	0.744 8(14)	
	−0.337(3)	−0.125 3(7)	0.735 5(17)	0.10(3)
H6b	−0.433(5)	−0.081 5(6)	0.561 0(14)	
	−0.442(3)	−0.073 5(9)	0.572(2)	0.15(2)

piezoelectric coefficients or resonance frequency.

It is known from the [13] that the FE hysteresis loops are slim between T_c and $T_{c'}$, while the electric field 16 kV cm^{-1} is not sufficient for the switching of the sample below $T_{c'}$. The drop of ε'_a near $T_{c'}$ was explained as resulting from domain wall freezing in [13]. However, the decrease of ε'_a due to the domain freezing cannot be sharp and it should be frequency dependent, as was shown for KH_2PO_4 and TGS single crystals [18]. In our case, only the value of ε'_a in the range of the plateau depends on the frequency; the temperature of the drop is not influenced. Also the temperature and pressure variation of the piezoelectric effect should be gradual in the case of domain freezing. The sudden change of piezoelectric constants (and thus of ε'_a) as well as the change of the (0, 12, 0) splitting (figure 3(*b*)) at $T_{c'}$ can therefore be

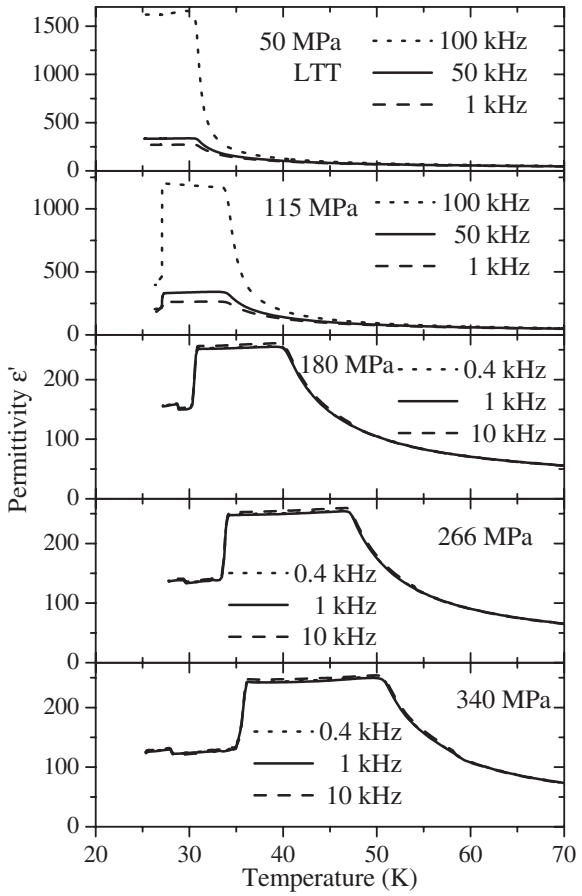

Figure 5. Temperature dependences of ε'_a obtained for five different hydrostatic pressures at several selected frequencies; the sample thickness and applied voltage were 600 μm and 1 V, respectively.

successfully explained only by assuming another FPT.

The FE phase below $T_{c'}$ is characterized by a larger monoclinic distortion than the phase between T_c and $T_{c'}$. A sharp drop of ε'_a at $T_{c'}$ provides evidence in support of first-order character of the isomorphous PT and of lower piezoelectricity in the phase below $T_{c'}$. Both FE phases remain monoclinic with the space group $P2_111$.

4. Conclusions

We have determined the crystal structures of the PE and lower FE phases in LTT at an applied hydrostatic pressure of 120 MPa, leading to an increase of the PE/FE transition temperature from 11 to 36 K. The results of the structure refinement suggest that the spontaneous polarization arises mainly from the displacements of Li atoms along the crystallographic a-axis. The accompanying studies of the thermal variation of the dielectric permittivity and of the monoclinic distortion angle of LTT with the applied pressure have revealed a new structural PT of first order at 27 K. Both of the low-temperature phases are monoclinic and FE but exhibit different distortion angles and different coefficients of the piezoelectric coupling.

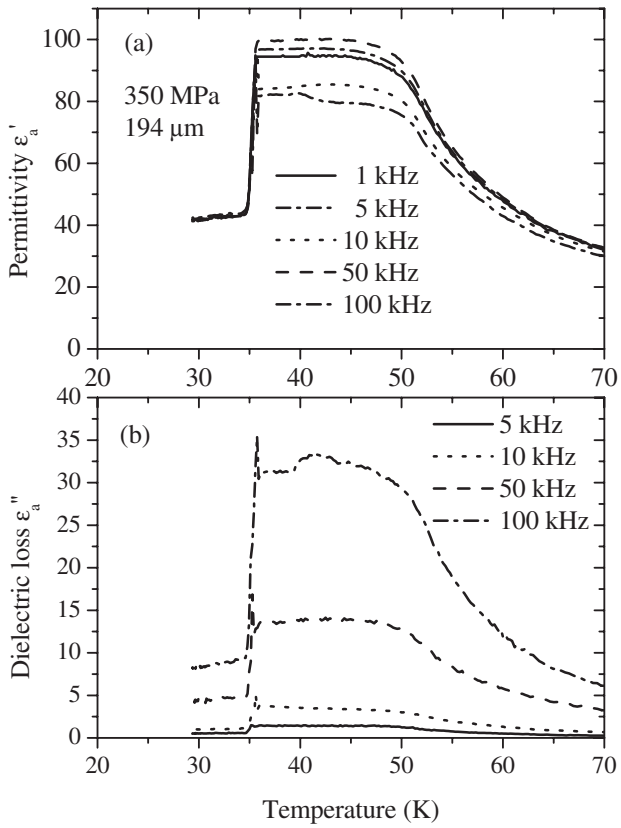

Figure 6. Temperature dependences of ε'_a and ε''_a obtained at 350 MPa for five different frequencies; the sample thickness was 194 μm.

Acknowledgments

The authors are grateful to B Březina for providing us with large LTT single crystals of excellent optical quality, to G Schaack for helpful discussion of high-pressure dielectric and Raman scattering data and to T Fernandez-Diaz for technical help with the neutron scattering experiment at ambient pressure. The work was supported by the Grant Agency of the Czech Republic (project No 202/01/0612) and the Grant Agency of the Academy of Sciences (project No A1010213).

References

[1] Suzuki E and Shiozaki Y 1996 *Phys. Rev.* B **53** 5217
[2] McCarthy G J, Schlegel L H and Sawaguchi E 1971 *J. Appl. Crystallogr.* **4** 180
[3] Kay M I 1978 *Ferroelectrics* **19** 159
[4] Valasek J 1921 *Phys. Rev.* **17** 475
[5] Mathias B T and Hulm J K 1951 *Phys. Rev.* **82** 108
[6] Fousek J, Cross L E and Seely K 1970 *Ferroelectrics* **1** 63
[7] Sawaguchi E and Cross L E 1971 *Ferroelectrics* **2** 37
[8] Abe R, Kamiya N and Matsuda M 1974 *Ferroelectrics* **8** 557
[9] Hayashi K, Deguchi K and Nakamura E 1992 *J. Phys. Soc. Japan* **61** 1357

[10] Deguchi K and Nakamura E 1993 *J. Phys. Soc. Japan* **62** 3392
[11] Březina B, Janoušek V, Mareček V and Smutny F 1970 *Proc. European Mtg on Ferroelectricity* ed H E Müsser and J Petersson (Stuttgart: Wissenschaftliche Verlagsgesselschaft) p 369
[12] Deguchi K and Iwata Y 2000 *J. Phys. Soc. Japan* **69** 135
[13] Kamba S, Schaack G, Petzelt J and Březina B 1996 *J. Phys.: Condens. Matter* **8** 4631
[14] Samara G A and Peercy P S 1981 *Solid State Physics; Advances in Research and Applications* vol 36, ed H Ehrenreich, F Seitz and D Turnbull (New York: Academic) p 1
[15] Volkov A A, Goncharov Yu G, Kozlov G V, Petzelt J, Fousek J and Březina B 1986 *Sov. Phys.–Solid State* **28** 1794
[16] Petříček V and Dušek M 2000 *Programs for Modulated and Composite Crystals* (Prague: Institute of Physics)
[17] Hlinka J, Kulda J, Kamba S and Petzelt J 2001 *Phys. Rev.* B **63** 052102
[18] Huang Y N, Wang Y N, Li X and Ding Y 1998 *J. Korean. Phys. Soc.* **32** S733